Leaf chlorophyll content estimation for Moso bamboo using hyperspectral reflectance

Zhen-bang Hao (1), Li-li Lin(1), Jian Liu(2), Kun-yong Yu(1),

[1] Fujian Agriculture and Forestry University, Fuzhou, Fujian 350002, China
[2] Sanming University, Sanming, Fujian 365001, China
Email: haozhenbang@outlook.com; fjlililin@126.com

Keywords: Moso bamboo; hyperspectral remote sensing; leaf chlorophyll content; canopy leaves

Abstract: Leaf chlorophyll content is closely related to plant health and nutritional status. Thus, the accurate and efficient estimates of leaf chlorophyll content are important for precision forestry. This study employed hyperspectral reflectance, which is robust and nondestructive to derive the leaf chlorophyll content of Moso bamboo. The spectral reflectance and chlorophyll content of corresponding leaves in 86 plots were determined by an ASD FieldSpec 4 field spectrometer and Thermo Scientific microplate reader, respectively. Correlation analysis was used to determine the most sensitive parameters of the original spectral reflectance, first derivative reflectance, spectral parameters, and vegetation index. These parameters were then used to construct leaf chlorophyll content model by unary model, multivariate linear model, random forest (RF), and support vector machines (SVM). The results indicated that (1) the reflectance at 562 nm, the first derivative reflectance at 650 nm, the normalized value of red edge and blue edge areas ((Sr-Sb)/(Sr+Sb)), and the chlorophyll absorption reflectance index (CARI) had the highest correlation with leaf chlorophyll content, respectively; (2) the power function model constructed using R562 nm and the leaf chlorophyll content yielded the highest R^2amongst 15 unary models. Then, using 562 nm, 650 nm, (Sr-Sb)/(Sr+Sb), and CARI as variables, a leaf chlorophyll content inversion model was established using the multivariate linear method, the coefficient of determination reached 0.716; RF and SVM, with R^2values were 0.870 and 0.763. Among them, RF had the best performance. This study demonstrates that RF is the best-fit model for estimating the leaf chlorophyll content of Moso bamboo. These results contribute towards the rapid and nondestructive determination of leaf chlorophyll content.

1. INTRODUCTION

Moso bamboo (*Phyllostachys pubescens*) is an important forest resource, and well known as an economic bamboo species with a high annual output of timber, rapid growth, and wide applications. Moreover, it plays an important role in the carbon cycle and water conservation. In China, the planted area of Moso bamboo is approximately 74% of the total bamboo forest area (Yang et al., 2019; Qin et al., 2017; Li et al., 2019). the threat of diseases and insect pests occurs in Moso bamboo growth areas, mostly spread from point to surface, that cause economic losses and difficult to control(Huang et al., 2018). Thus, requires to examine and monitor bamboos growth is necessary.

Leaf chlorophyll content is an important indicator of plant photosynthesis, nutritional status, and growth position(Sonobe et al., 2017; Yang et al., 2015). Changes in the leaf chlorophyll content are related to environmental stress, pests, and diseases(Féret et al., 2017); therefore, accurate estimates of leaf chlorophyll content are highly significant for monitoring vegetation growth and nutrients. In crop fields (i.e. corn, wheat, and potato), hyperspectral remote sensing has been widely used to monitor and estimate chlorophyll content(Zhao et al., 2013; Kjær et al., 2017; Li et al., 2017). Spectral data is also required to obtain vegetation growth information in precision forestry. However, field sampling surveys are difficult; specifically, sometimes spectral data is required by erecting towers at different heights.

Leaf chlorophyll content estimation using hyperspectral remote sensing involves both physical and empirical models(Sonobe et al., 2017; Zhao et al., 2013). Among existing physical models, the PROSPECT model is a commonly used leaf-level radiative transfer model(Sun et al., 2018) that simulates inversion spectra based on the leaf and other properties. However, it has some parameters that are difficult to obtain. And, although it is more popular for estimating chlorophyll content, it involves certain assumptions in order to simplify the complexities of nature. Moreover, it cannot be applied to conifer needle leaves(Sun et al., 2019). Conversely, a large number of studies have analyzed the empirical relationship between measured leaf chlorophyll content and spectral features(Richardson et

al., 2002; Lausch et al., 2015). There are two commonly used spectral features: one is spectral indices, including the spectral reflectance, derivative reflectance, and vegetation index, and the other is the characteristic spectral position variable, including the red edge position, etc.(Li et al., 2017; Peng et al., 2018; Zhou et al., 2019). Compared with the PROSPECT model, spectral features are convenient and may have general applicability for large-scale monitoring(Sonobe et al., 2017).

Machine learning algorithms (MLAs) represent a new field of model construction, that includes random forest (RF), support vector machine (SVM), and artificial neural network (ANN) models. Applications of these models include landslide detection(Ghorbanzadeh et al., 2019), forest parameter estimation(Zhao et al., 2019), and so on. MLAs have excellent learning and prediction ability in data analysis and can be easily applied to functional regression problems(Cooner et al., 2016). Moso bamboo is predominantly distributed in hilly and mountainous areas; therefore, it is difficult to detect the leaf chlorophyll content. Moreover, a limited study was carried out to compare MLAs with empirical models, which one provides better accuracy in the leaf chlorophyll content evaluation of Moso bamboo.

Therefore, this study explores the optimal method for estimating the leaf chlorophyll content of Moso bamboo using hyperspectral remote sensing. First, we retrieve vegetation indices form hyperspectral data and determine the leaf chlorophyll content. Second, we analyze the spectral characteristics of chlorophyll and reveal the hyperspectral response of leaf chlorophyll content. Lastly, we develop an inversion model to determine the leaf chlorophyll content of Moso bamboo based on different parameters, then select the optimal approach for estimating leaf chlorophyll content.

2. MATERIALS AND METHODS

2.1. Study area

The study site is located in Fujian Tianbaoyan National Nature Reserve, Yong'an City, Fujian Province, China (117°28'3"~117°35'28"E, 25°50'51"~26°1'20" N) (Fig. 1). Elevations vary from 580 m to 1604.8 m above mean sea level. The site is characterized by a subtropical maritime monsoon climate zone with an average annual temperature of 15 °C. The average annual precipitation is 2039 mm and concentrated from May- September, and the average annual relative humidity is over 80%. A highly intensive plantation of Moso bamboo forest is located in the experimental area. The site area is a forest ecological protection zone, which has high scientific research value and a forest coverage rate of 96.8%.

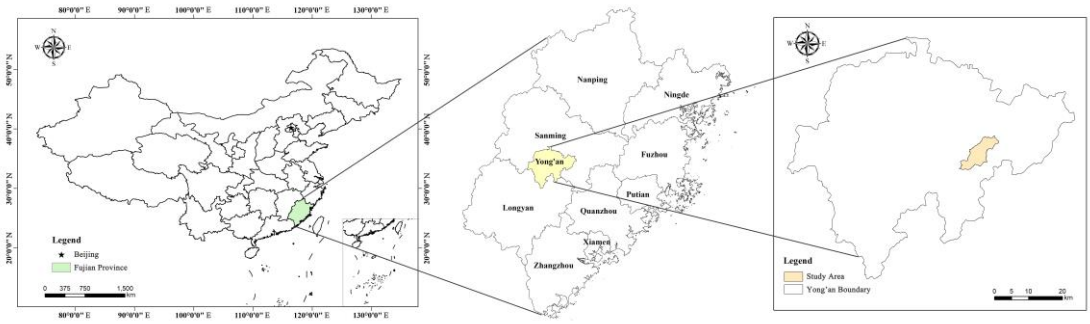

Fig. 1. Location of the study site

2.2. Experimental design

The experiment comprises two main parts: (1) measurement of the spectral reflectance and chlorophyll content of Moso bamboo and (2) determining the relationship between spectral reflectance and chlorophyll content. To measure the spectral characteristics of Moso bamboo leaves, 86 plots were established in Fujian Tianbaoyan National Nature Reserve. The size of each plot was 25.8 m × 25.8 m. The reflectance values and leaf chlorophyll content of the upper, middle, and lower layers of Moso bamboo canopy were obtained separately.

2.3. Spectral reflectance and chlorophyll content measurement

The spectral reflectance of Moso bamboo was measured from August 15 to September 16, 2018 during on-years (years with great shoot production), using a spectrometer (FieldSpec4, Analytical Spectral Devices Inc., USA). The spectral range of the spectrometer was 350 nm to 2500 nm, with a spectral resolution of 3 nm between 350 nm and 1400 nm and 6 nm between 1400 nm and 2100 nm. The reflectance of the blade was measured directly by a spectrometer with a built-in halogen tungsten lamp. A standard bamboo plant was cut down in each sample plot and

nine leaves were randomly selected from each layer to determine the spectrum. A total of 27 leaves were determined for each tree.

After measuring the spectral reflectance, the leaves were immediately stored in a heat preservation box and brought back to the laboratory to determine the chlorophyll content. First, nine leaves of the same layer were cut, and 0.05 g samples were placed into a centrifugal tube with 8 ml of extract (acetone: anhydrous ethanol = 3:1). Next, the centrifugal tube was immersed in a dark environment for 48 h and shaken every 12 h(Wang et al., 2015). After the leaves turned white, the absorbance of the chlorophyll solution at 663 nm and 645 nm was measured using a Thermo Scientific enzyme-labelling measuring instrument. Each sample was measured three times for leaf chlorophyll content. Finally, the chlorophyll content was calculated using

$$C_t = {1000(17.18A_{663} + 17.32A_{646})V}/{M} \quad (1)$$

where C_t is the fresh leaf chlorophyll content (mg/g), V is the total volume of the extract (8 ml), and M is the leaf extraction amount (0.05 mg).

2.4. Model construction

2.4.1. Data preprocessing

The data was pre-processed with the ViewSpecPro software of the ASD FieldSpec 4 spectrometer. The mean value of nine leaves per layer was used as the leaf reflectance of that layer.

2.4.2. Selection and construction of chlorophyll-related indicators

To determine the sensitive band for the leaf chlorophyll content of Moso bamboo, we used SPSS software to analyze the correlation between leaf chlorophyll content and original spectral reflectance, first derivative reflectance after pretreatment. The most relevant wavelength was selected as the sensitive wavelength for subsequent modeling.

Among the vegetation indices recorded in the literature(Yang et al., 2015; Zhou et al., 2019; Xue et al., 2009; Le Maire et al., 2004), 28 published hyperspectral vegetation indices and ten types of spectral parameter were selected for model construction; these parameters included the blue edge amplitude (Db), blue edge position (λb), red valley amplitude (Rr), red valley position (λv), red edge amplitude (Dr), red edge position (λr), red edge Area (Sr), blue edge area (Sb), red edge area to blue edge area ratio (Sr/Sb), red edge area and blue edge area normalized value ((Sr-Sb)/(Sr+Sb)). Based on the results of the correlation analysis, the maximum correlation spectral parameter and vegetation index were chosen for further analysis.

2.4.3. Model construction and accuracy evaluation

253 sample data were obtained and randomly divided into 202 samples for the modeling set and 51 samples for the validation set, with a ratio of 4:1. The most relevant correlation of the original spectral reflectance, first derivative reflectance, spectral parameters, and vegetation index were selected to construct the chlorophyll inversion model. A variate linear model was built using Excel software, and a multivariate linear model was built using SPSS software. Random forest (RF) classification and support vector regression (SVR) were performed using Python 3.0 software.

The coefficient of determination (R^2), the root mean square error (RMSE), and the relative error (RE) were used to evaluate the accuracy of the inversion models(Li et al., 2017):

$$R^2 = \frac{\sum_{i=1}^{n}(\hat{y}-\bar{y})^2}{\sum_{i=1}^{n}(y-\bar{y})^2} \quad (2)$$

$$RMSE = \sqrt{\frac{1}{n}\sum_{i=1}^{n}(\hat{y}-y)^2} \quad (3)$$

$$RE = \frac{1}{n}\sum_{i=1}^{n}\left(\frac{\left|\hat{y}-y\right|}{y} \times 100\%\right) \quad (4)$$

where y is the measured value of the sample, $\hat{y}$ is the estimated value of the sample, $\bar{y}$ is the average value of the measured sample, and n is the number of samples. The smaller the values of RMSE and RE, the higher the accuracy of the model, and the better the correlation between measured and estimated values.

3. RESULTS

3.1. Correlation analysis

3.1.1 Correlation between chlorophyll content, original reflectance, and first derivative reflectance

The highest correlations between chlorophyll content and original spectral reflectance of Moso bamboo leaves were 409-752 nm, 1708-1776 nm and 2270-2450 nm (Fig. 2). The original spectral reflectance for 409-752 nm exhibited a highly significant negative correlation with the chlorophyll content (p<0.01). Moreover, significant positive correlations were confirmed between chlorophyll content and reflectance values for 1708-1776 nm and 2270-2450 nm (p<0.05). The highest correlation was obtained at 562 nm (R562 nm), for which the correlation coefficient was -0.827. Thus, 562 nm was selected as the independent candidate variable for the modeling parameter.

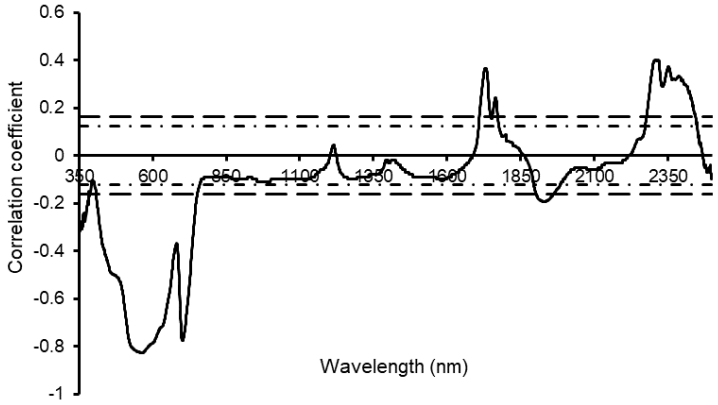

Fig.2 Curve of the correlation coefficient between chlorophyll content and the original spectral reflectance of Moso bamboo leaves

The highest correlation between chlorophyll content and the first derivative reflectance of Moso bamboo leaves was predominantly in the visible band (Fig. 3). There was a strong negative correlation for 484-552 nm and 683-718 nm, and a significant positive correlation for 554-679 nm (p<0.05). The derivative reflectance at DR 650 nm had the highest correction with chlorophyll content, with a correlation coefficient of 0.791. Therefore, DR 650 nm was selected the modeling parameter for the first derivative reflectance.

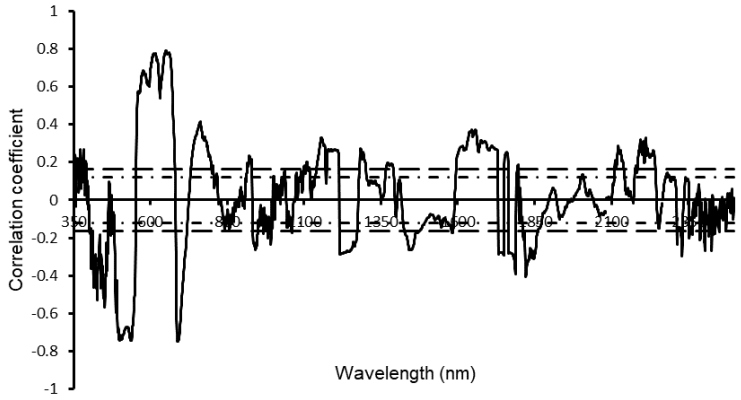

Fig.3 Curve of the correlation coefficient between chlorophyll content and the first derivative reflectance of Moso bamboo leaves

3.1.2. Correlation between chlorophyll content and hyperspectral parameters

The red edge position (λr), red valley position (λv), red valley amplitude (Rr), blue edge position (λb), blue edge amplitude (Db), blue edge area (Sb), red edge area to blue edge area ratio (Sr/Sb), and normalized value of red edge area and blue edge area ((Sr-Sb)/(Sr+Sb)) exhibited a highly significant relationship with leaf chlorophyll content (Table 1). Among them, the correlation coefficient between the normalized value of red edge area and blue edge area ((Sr-Sb)/(Sr+Sb)) and chlorophyll content was the highest, at 0.740. Conversely, the red edge amplitude (Dr) and red edge area (Sr) exhibited no correlation with leaf chlorophyll content. Therefore, we chose the normalized value of red edge area and blue edge area ((Sr-Sb)/(Sr+Sb)) as the modeling parameter.

Table 1 Correlations between chlorophyll content and hyperspectral parameters

Hyperspectral parameters	Correlation coefficient
λr	0.458**
Dr	0.108
λv	-0.651**
Rr	-0.449**
λb	0.184**
Db	-0.679**
Sr	-0.067
Sb	-0.716**
Sr/Sb	0.717**
(Sr-Sb)/(Sr+Sb)	0.740**

Note: * is a significant level (p < 0.05), **is a highly significant level (p < 0.01).

3.1.3. Correlations between chlorophyll and vegetation indices

Correlation analysis of the hyperspectral vegetation indices and leaf chlorophyll content yielded high Pearson correlation values for a majority of the vegetation indices (Table 2). Among them, 25 vegetation indices had highly significant correlations with chlorophyll content. The five vegetation indices with the highest correlation with chlorophyll content were RVI II, SIPI, CARI, GNDVI, and $GNDVI_{801\text{-}550}$. The correlation between CARI and chlorophyll content was the highest, with a correlation coefficient of -0.785. Conversely, VI opt, NDPI, RVSI exhibited no correlation with leaf chlorophyll content. Thus, CARI was used as the vegetation index when building the model.

Table 2. Chlorophyll-sensitive vegetation spectral index

Vegetation indices	Algorithm	Pearson correlation
Optimal vegetation index (VIopt)	$(1+0.45)(R_{800}^2+1)/(R_{670}^2+0.45)$	0.031
Normalized difference vegetation index g-b (NDVI g-b)	$(R_{575}-R_{440})/(R_{575}+R_{440})$	-0.514**
Ratio vegetation index I (RVI I)	R_{810}/R_{660}	0.486**
Ratio vegetation index II (RVI II)	R_{801}/R_{560}	0.741**
Modified chlorophyll absorption reflectance index MCARI/MTVI2	MCARI=$R_{700}-R_{670}-0.2(R_{700}-R_{550})(R_{700}/R_{670})$ $MTVI_2$=$1.5[1.2(R_{800}-R_{550})-2.5(R_{670}-R_{500})]/$ sqrt$[2(2R_{800}+1)-(6R_{8000}-5\text{sqrt}(R_{670}))-0.5]$	-0.660**
Doublet canopy nitrogen index (DCNI)	$(R_{720}-R_{700})/(R_{700}-R_{670})/(R_{720}-R_{670}+0.03)$	0.657**
Transformation chlorophyll absorption reflectance index/Optimized soil-adjusted vegetation index (TCARI/OSAVI)	TCARI=$3[R_{700}-R_{670}-0.2(R_{700}-R_{550})](R_{720}/R_{670})$ OSAVI=$1.16(R_{800}-R_{670})(R_{800}+R_{670}+0.16)$	-0.505**
MERIS terrestrial chlorophyll index (MTCI)	$(R_{750}-R_{710})/(R_{710}-R_{680})$	0.630**
R-M	$R_{750}/R_{720}-1$	0.594**
Senescence reflectance index (SRI)	R_{801}/R_{670}	0.390**
Spectral reflectance index (SR705)	R_{750}/R_{705}	0.615**
Normalized difference pigment index (NDPI)	$(R_{680}-R_{430})/(R_{680}+R_{430})$	0.015
Structure intensive pigment index (SIPI)	$(R_{800}-R_{445})/(R_{800}-R_{550})$	-0.741**
Chlorophyll absorption reflectance index (CARI)	$\frac{\lvert 670a+R_{670}+b\rvert R_{700}}{\sqrt{a^2+1}\times R_{670}}$ a=$(R_{700}-R_{550})/150$，b=$R_{550}-500a$	-0.785**
Plant senescence reflectance index (PSRI)	$(R_{680}-R_{500})/R_{750}$	0.595**
Vogelmann red edge index (VOGB)	$(R_{734}-R_{747})/(R_{715}+R_{726})$	-0.582**
Vogelmann red edge index (VOGC)	$(R_{734}-R_{747})/(R_{715}+R_{720})$	-0.587**
Red edge NDVI (rNDVI)	$(R_{750}-R_{705})/(R_{750}+R_{705})$	0.598**
Green normalized difference vegetation (GNDVI)	$(R_{750}-R_{550})/(R_{750}+R_{550})$	0.712**
Photochemical reflectance index (PRI)	$(R_{531}-R_{570})/(R_{531}+R_{570})$	0.550**
Red-edge vegetation stress index (RVSI)	$(R_{712}+R_{715})/2-R_{732}$	0.040
PSND	$(R_{800}-R_{470})/(R_{800}+R_{470})$	0.358**
PPR	$(R_{550}-R_{450})/(R_{550}+R_{450})$	-0.397**
MSR	$(\frac{R_{800}}{R_{670}}-1)/sqrt(\frac{R_{800}}{R_{670}}+1)$	0.364**
Normalized difference vegetation index800-680 (NDVI800-680)	$(R_{800}-R_{680})/(R_{800}+R_{680})$	0.233**
Normalized difference vegetation index503-483 (NDVI503-483)	$(R_{503}-R_{483})/(R_{503}+R_{483})$	-0.517**
Normalized difference vegetation index801-550 (NDVI801-550)	$(R_{801}-R_{550})/(R_{801}+R_{550})$	0.729**

The reflectance value at wavelength (nm).

3.2. Modeling results

3.2.1. Results of the unary model based on different parameters

The inversion models of R562 nm, DR650 nm, (Sr-Sb)/ (Sr+Sb), and CARI with leaf chlorophyll content were constructed using monadic linear, quadratic curve, exponential, and power function models, respectively. According to Table 3, the power coefficient model of R562 nm showed the best fitting effect, with the highest coefficient of determination (R^2=0.739, RMSE=0.431, RE=10.93%). The model inversion accuracy was similar for DR650 nm and CARI, regardless of the type of model (the power function model of DR650 nm was excluded). And the coefficient

of determination was 0.600-0.700, which was lower than the model constructed using R562 nm. The four models using (Sr-Sb)/ (Sr+Sb) as parameter had the lowest inversion accuracy, all of which were less than 0.5.

Table 3. Construction and accuracy evaluation of unary model

Parameters	Model	Regression equation	Coefficient of determination (R^2)	Root mean square error (RMSE)	Relative error (RE) /%
R562	Monadic linear model	$y = -44.67x + 9.5969$	0.703	0.419	10.68%
	Quadratic curve model	$y = 212.72x^2 - 101.56x + 13.352$	0.703	0.420	10.64%
	Exponential model	$y = 18.971e^{-12.58x}$	0.718	0.422	10.62%
	Power function model	$y = 0.1252x^{-1.654}$	0.739	0.431	10.96%
DR650	Monadic linear model	$y = 5323.1x + 6.3045$	0.627	0.496	12.68%
	Quadratic curve model	$y = -632541x^2 + 4688.8x + 6.155$	0.636	0.498	12.72%
	Exponential model	$y = 7.5355e^{1507.3x}$	0.607	0.500	12.29%
	Power function model	The first order differential is negative, so there is no power function model.			
(Sr-Sb)/ (Sr+Sb)	Monadic linear model	$y = 28.501x - 20.612$	0.457	0.527	12.43%
	Quadratic curve model	$y = -29.209x^2 + 78.236x - 41.77$	0.471	0.530	12.56%
	Exponential model	$y = 0.0037e^{8.0822x}$	0.443	0.520	11.98%
	Power function model	$y = 10.802x^{6.8907}$	0.442	0.526	11.85%
CARI	Monadic linear model	$y = -44.938x + 8.3954$	0.671	0.464	12.12%
	Quadratic curve model	$y = 266.13x^2 - 101.55x + 11.351$	0.664	0.457	11.72%
	Exponential model	$y = 13.481e^{-12.63x}$	0.672	0.459	11.54%
	Power function model	$y = 0.1843x^{-1.311}$	0.694	0.463	11.64%

3.2.2. Results of other models

Figure 4 shows the relationships between measured and predicted chlorophyll content. The coefficient of determination (R^2) for the multivariate liner model constructed using 562 nm, 650 nm, (Sr-Sb)/(Sr+Sb), and CARI as parameters was 0.716, RMSE was 0.412, and RE was 8.71%. The model yielded the following estimation formula:

y=-26.278*R562+1854.277*DR650+1.481*(Sr-Sb)/(Sr+Sb)-3.966* CARI+7.228

The RF algorithm and SVM were constructed using Python. The R^2 value of the RF model and radial basis kernel function SVM model were 0.870 (RMSE=0.378, RE =8.21% and 0.763 (RMSE=0.372, RE =8.44%) (Fig. 4). A comparison of the measured and simulated datasets revealed that RF can more accurately derive the leaf chlorophyll content of Moso bamboo.

Except for the exponential model and power function model constructed using the original spectral reflectance, R562 nm, the R^2 of the multivariate model constructed by multivariate linear, RF, and SVM was greater than 0.7, which was superior to the unary model constructed using the original spectral reflectance, first derivative reflectance, spectral parameters, and vegetation index. Moreover, the RMSE value was lower than that for the unary model.

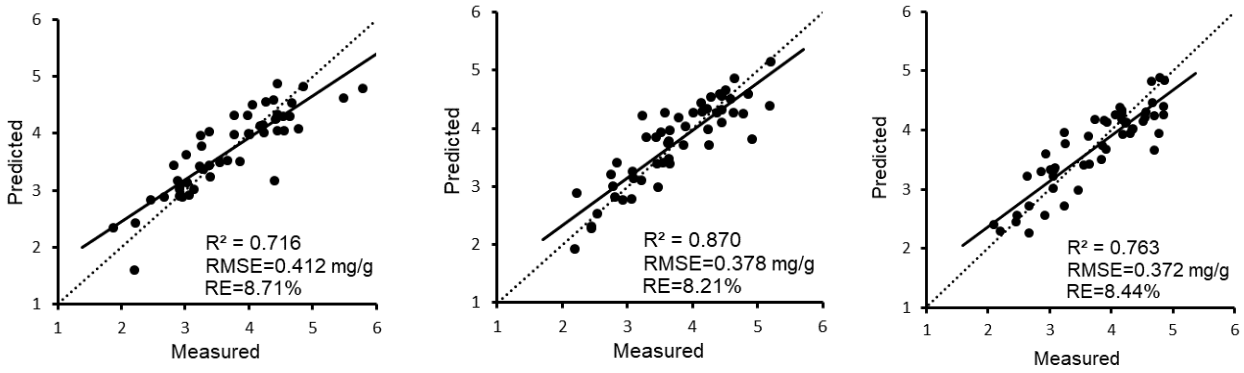

Fig.4 Verification of measured and predicted chlorophyll content by the multivariate liner model (a), random forest model (b), and radial basis kernel function support vector machine model (c)

4. DISCUSSION

4.1 Spectral characteristics of Moso bamboo

Moso bamboo exhibits dynamic growth changes. At different bamboo ages, the leaf chlorophyll content displays substantial differences. Additionally, Moso bamboo is typified by high shoot production during on-years and the growth of whips and replacement of bamboo leaves during off-years. Guan et al.(2012) indicated that on-year bamboo presented “two humps” in spring and summer (Guan et al., 2012). Although our study did not reveal this phenomenon, it is consistent with other research indicating that the visible and near-infrared spectrum is more sensitive to leaf chlorophyll content(Huang et al., 2018; Blackburn et al., 1998). There are three spectral reflectance bands that are sensitive to chlorophyll content: 409-752 nm, 1708-1776 nm, and 227-2450 nm. Among them, the correlation between spectral reflectance and chlorophyll content is the highest in the visible band, reaching a maximum at 562 nm.

4.2. Effect of model development

Our study divided the bamboo canopy into upper, middle, and lower layers, and measured the corresponding leaf chlorophyll content. It can reasonable to deduce Figure 5 indicates that the chlorophyll content of Moso bamboo leaves varied among different canopy layers. Compared with other research on plant leaves (e.g. maize and rice)(Kjær et al., 2017), our sampling method is more representative and improves the estimation accuracy of the leaf chlorophyll content of Moso bamboo.

Subsequently, due to the influence of the spectrometer itself and the moisture in the atmosphere, the measured spectral curve of vegetation will produce irregular vibrations as the wavelength increases(Wang et al., 2018). This noise will affect the accuracy of vegetation information extraction. In this study, a portable system with Field Spec4 was used for spectral determination, and a built-in light source was used as the light source. This can effectively reduce the effect of interference from the environment and changes in light under the forest on the spectral reflectance measurement. The traditional approach requires tremendous effort for sample collection and laboratory chemical analyses(Sonobe et al., 2017). Moreover, the process of measuring chlorophyll is destructive and does not allow rapid and effective monitoring on large scale. Thus, hyperspectral remote sensing is valuable as a rapid and nondestructive method for estimating leaf chlorophyll content. Soil Plant Analysis Development (SPAD), it another spectroscopic method used to determine the relative content of chlorophyll with a portable chlorophyll analyzer. However, the band used to estimate the chlorophyll content is single and fixed, which is not appropriate for large-area measurement(Agarwal et al., 2018). Conversely, this study employed linear and non-linear algorithms to determine the optimal method for deriving the leaf chlorophyll content of Moso bamboo.

4.3 Research prospects

This research explores a more accurate estimation method for the leaf chlorophyll content of Moso bamboo. Although we consider upper, middle, and lower canopy layer, we focus on the leaf level, with no extension to the canopy scale. Thus, considering the leaf and canopy scale effect, several leaf-canopy radiative transfer models should be applied in future(Le Maire et al., 2004). The method proposed on this study can be used to rapidly and precisely derive the special reflectance of Moso bamboo, which differ from that of other typical vegetation(Guan et al., 2012;

Zhang et al., 2016).

5. CONCLUSIONS

This study analyzed the correlation between the chlorophyll content of Moso bamboo and the original spectral reflectance, first derivative reflectance, spectral parameters, and vegetation indices in order to determine the spectral variables with the highest correlation to bamboo chlorophyll content, and construct unary and multivariate inversion models of chlorophyll content. Through a comparative analysis, we drew the following conclusions:

(1) The most sensitive band intervals were 409-752 nm, 1708-1776 nm, and 2270-2450 nm in original spectral reflectance and 484-552 nm and 683-718 nm in first derivative reflectance. The majority of hyperspectral parameters and vegetation indices had a strong relationship with leaf chlorophyll content.

(2) Dfferent modeling methods exhibited different correlations (R^2) for leaf chlorophyll content estimates. Overall, RF exhibited better performance in terms of leaf chlorophyll content, with R^2 values of 0.870.

ACKNOWLEDGEMENTS

This work was supported by the National Key Research and Development Projects of P.R. China [grant number: 2018YFD060010304].

REFERENCES

Agarwal A., Dutta Gupta S., 2018. Assessment of spinach seedling health status and chlorophyll content by multivariate data analysis and multiple linear regression of leaf image features. Computers and Electronics in Agriculture, 152, pp. 281-289.

Blackburn G. A., 1998. Spectral indices for estimating photosynthetic pigment concentrations: A test using senescent tree leaves. International Journal of Remote Sensing, 19(4), pp. 657-675.

Cooner A., Shao Y., Campbell J., 2016. Detection of urban damage using remote sensing and machine learning algorithms: Revisiting the 2010 haiti earthquake. Remote Sensing, 8(10), pp. 868.

Féret J. B., Gitelson A. A., Noble S. D., 2017. Jacquemoud S. PROSPECT-D: Towards modeling leaf optical properties through a complete lifecycle. Remote Sensing of Environment, 193, pp. 204-215.

Guan F., Deng W., Fan S., 2012. Spectral characteristics of Phyllostachys pubescens stand and its differential analysis with typical vegetation. Journal of Beijing Forestry University, 34(03), pp. 31-35.

Huang X., Xu Z., Lin L., Liu J., Zhong Z., Zhou H., 2018. Spectral characteristic wavelengths of moso bamboo leaves damaged by pantana phyllostachysae chao. Spectroscopy and Spectral Analysis, 38(12), pp. 3829-3838.

Kjær A., Nielsen G., Stærke S., Clausen M. R., Edelenbos M., Jørgensen B., 2017. Detection of Glycoalkaloids and Chlorophyll in Potatoes (Solanum tuberosum L.) by Hyperspectral Imaging. American Journal of Potato Research, 94(6), pp. 573-582.

Lausch A., Salbach C., Schmidt A., Doktor D., 2015. Merbach I., Pause M. Deriving phenology of barley with imaging hyperspectral remote sensing. Ecological Modelling, 295, pp. 123-135.

Li D., Cheng T., Zhou K., Zheng H., Yao X., Tian Y., Zhu Y., Cao W., 2017. WREP: A wavelet-based technique for extracting the red edge position from reflectance spectra for estimating leaf and canopy chlorophyll contents of cereal crops. ISPRS Journal of Photogrammetry and Remote Sensing, 129, pp. 103-117.

Li L., Li N., Lu D., Chen Y., 2019. Mapping Moso bamboo forest and its on-year and off-year distribution in a subtropical region using time-series Sentinel-2 and Landsat 8 data. Remote Sensing of Environment, 231:111265.

Le Maire G., François C., Dufrêne E., 2004. Towards universal broad leaf chlorophyll indices using PROSPECT simulated database and hyperspectral reflectance measurements. Remote Sensing of Environment, 89(1), pp. 1-28.

Peng Y., Fan M., Wang Q., Lan W., Long Y., 2018. Best hyperspectral indices for assessing leaf chlorophyll content in a degraded temperate vegetation. Ecology and Evolution, 8(14), pp. 7068-7078.

Qin H., Niu L., Wu Q., Chen J., Li Y., Liang C., Xu Q., Fuhrmann J. J., Shen Y., 2017. Bamboo forest expansion increases soil organic carbon through its effect on soil arbuscular mycorrhizal fungal community and abundance. Plant and Soil, 420(1-2), pp. 407-421.

Richardson A. D., Duigan S. P., Berlyn G. P., 2002. An evaluation of noninvasive methods to estimate foliar chlorophyll content. New Phytologist.

Sonobe R., Wang Q., 2017. Hyperspectral indices for quantifying leaf chlorophyll concentrations performed differently with different leaf types in deciduous forests. Ecological Informatics, 37, pp. 1-9.

Sun J., Shi S., Yang J., Chen B., Gong W., Du L., Mao F., Song S., 2018. Estimating leaf chlorophyll status using

hyperspectral lidar measurements by PROSPECT model inversion. Remote Sensing of Environment, 212, pp. 1-7.
Sun J., Shi S., Yang J., Gong W., Qiu F., Wang L., Du L., Chen B., 2019. Wavelength selection of the multispectral lidar system for estimating leaf chlorophyll and water contents through the PROSPECT model. Agricultural and Forest Meteorology, 266-267, pp. 43-52.
Ghorbanzadeh O., Blaschke T., Gholamnia K., Meena S., Tiede D., Aryal J., 2019. Evaluation of different machine learning methods and Deep-Learning convolutional neural networks for landslide detection. Remote Sensing, 11(2):196.
Wang J., Wu W., Wang T., Cai C., 2018. Estimation of leaf chlorophyll content and density inPopulus euphratica based on hyperspectral characteristic variables. Spectroscopy Letters, 51(9), pp. 485-495.
Wang X., Huang J., 2015. Principles and techniques of plant physiological biochemical experiment. Beijing: Higher Education Press, pp. 308.
Xue L., Yang L., 2009. Deriving leaf chlorophyll content of green-leafy vegetables from hyperspectral reflectance. ISPRS Journal of Photogrammetry and Remote Sensing, 64(1), pp. 97-106.
Yang C., Ni H., Zhong Z., Zhang X., Bian F., 2019. Changes in soil carbon pools and components induced by replacing secondary evergreen broadleaf forest with Moso bamboo plantations in subtropical China. Catena, 180, pp. 309-319.
Yang X. G., Yu Y., Fan W. Y., 2015. Chlorophyll content retrieval from hyperspectral remote sensing imagery. Environmental Monitoring and Assessment, 187(7).
Zhao K., Valle D., Popescu S., Zhang X., Mallick B., 2013. Hyperspectral remote sensing of plant biochemistry using Bayesian model averaging with variable and band selection. Remote Sensing of Environment, 132, pp. 102-119.
Zhao Q., Yu S., Zhao F., Tian L., Zhao Z., 2019. Comparison of machine learning algorithms for forest parameter estimations and application for forest quality assessments. Forest Ecology and Management, 434, pp. 224-234.
Zhou X., Huang W., Zhang J., Kong W., Casa R., Huang Y., 2019. A novel combined spectral index for estimating the ratio of carotenoid to chlorophyll content to monitor crop physiological and phenological status. International Journal of Applied Earth Observation and Geoinformation, 76, pp. 128-142.
Zhang Y., Zhang X., Wang S., Li H., Xue S., 2016. Spectral reflectance characteristics of canopies of main tree species in Jingle forest farm in Fujian. Journal of Northwest a&F University, 44(02), pp. 83-89.